J|A|C|S ARTICLES

Published on Web 07/21/2009

# Directed Assembly of PEGylated-Peptide Coatings for Infection-Resistant Titanium Metal

Xiaojuan Khoo,[†] Paul Hamilton,[‡] George A. O'Toole,[§] Brian D. Snyder,[||] Daniel J. Kenan,[⊥] and Mark W. Grinstaff*,[†]

*Departments of Biomedical Engineering and Chemistry, Boston University, Boston, Massachusetts 02215, Affinergy, Inc., Durham, North Carolina 27713, Department of Microbiology and Immunology, Dartmouth Medical School, Hanover, New Hampshire 03755, Department of Orthopedic Surgery, Children's Hospital, Harvard Medical School, Boston, Massachusetts 02215, and Department of Pathology, Duke University Medical Center, Durham, North Carolina 27710*

Received March 17, 2009; E-mail: mgrin@bu.edu



***Abstract:*** Appropriate surface chemistry between a material and its surrounding biological environment is crucial to the eventual integration and performance of any implant, whether metal, plastic, or ceramic. A robust peptide-based coating technology capable of easily modifying the surface of titanium (Ti) metal through noncovalent binding is described. A short peptide possessing affinity for Ti was identified using a phage display screening process and subjected to an amino acid substitution exercise using solid-phase chemical synthesis. Through these studies, the HKH tripeptide motif was elucidated as an important contributor to Ti binding within the Ti-binding peptide. This peptide spontaneously and selectively adsorbs onto a Ti surface from dilute aqueous solution with submicromolar binding affinities as determined by ELISA and quartz crystal microbalance with dissipation monitoring (QCM-D), through a process largely dominated by electrostatic interactions. Atomic force microscopy (AFM) reveals a densely packed peptide adlayer with an average height of ~0.5 nm. Subsequently, a PEGylated analogue of the peptide was shown to rapidly coat Ti to afford a nonfouling surface that efficiently blocked the adsorption of fibronectin and significantly reduced the extent of *Staphylococcus aureus* attachment and biofilm formation *in vitro*. These PEGylated-peptide coatings show promise in terms of resolving two major hurdles common to implanted metals: (i) nonspecific protein adsorption and (ii) bacterial colonization. At the same time, the facile one-step modification process will facilitate the point-of-care application of these coatings in the surgical suite.

## Introduction

Nonspecific adsorption of proteins and cells at the material surface can trigger adverse biological responses, resulting in suboptimal device performance in terms of efficacy, longevity, and safety.[1,2] Bacterial infections are the second most commonly attributed cause of orthopedic implant failure, occurring in 1−2% of total hip and knee prostheses, 10% of fracture fixator devices, and nearly 85% of all external fixators.[3−5] In fact, it is estimated that over 50% of hospital-acquired infections are associated with implants and other indwelling medical devices.[6] When one considers the large numbers and increasing utilization of these devices, the importance of identifying a nonfouling coating that prevents unfavorable biological interactions is evident.

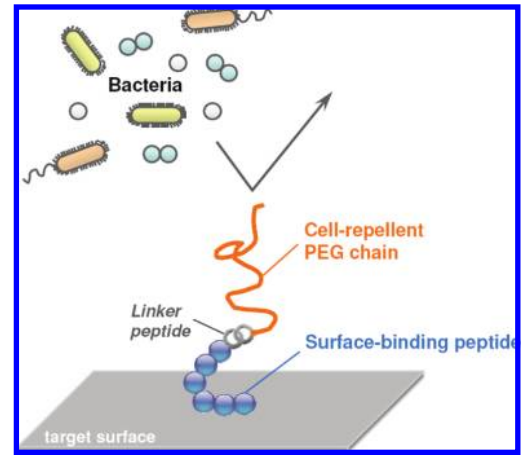


***Figure 1.*** Schematic of the nonfouling coating on a target surface. The coating comprises a surface-binding peptide (blue) linked to a cell-repellent poly(ethylene glycol) (PEG) chain (orange).

[†] Boston University.
[‡] Affinergy, Inc.
[§] Dartmouth Medical School.
[||] Harvard Medical School.
[⊥] Duke University Medical Center.

(1) Ratner, B. D.; Hoffman, A. S.; Schoen, F. J.; Lemons, J. E. *Biomaterials Science: An Introduction to Materials in Medicine*; Academic Press: San Diego, 2000.
(2) Williams, D. F. *Biomaterials* **2008**, *29*, 2941–2953.
(3) Kurtz, S.; Mowat, F.; Ong, K.; Chan, N.; Lau, E.; Halpern, M. *J. Bone Joint Surg. Am.* **2005**, *87*, 1487–1497.
(4) Sims, M.; Saleh, M. *Prof. Nurse* **1996**, *11*, 261–264.
(5) Davis, P. *Nursing Times* **2003**, *99*, 46–48.
(6) Stamm, W. E. *Ann. Intern. Med.* **1978**, *89*, 764–769.


**10.1021/ja9020827 CCC: $40.75** 

A commonly employed method for generating surfaces highly resistant to biofouling is to immobilize poly(ethylene glycol) (PEG), a nontoxic hydrophilic polyether, on biomaterial surfaces. High surface density PEG coatings form "brushlike" structures that prevent proteins from penetrating the substrate surface and shields secondary adsorption onto the outer surface of the PEG layer.[7] Current coating strategies include self-assembled monolayers (SAMs),[8−11] covalent grafting,[12−14] plasma deposition,[15] polyelectrolytes,[16,17] and bioadhesive protein mimics.[18−20] There exists a growing need for new coating strategies that enable rapid and facile modification without the need for surface pretreatments or harsh reaction conditions, especially those amenable to point-of-care application in the surgical setting. Few generalized methods for accomplishing this have been previously reported. Herein, we describe the design of a novel PEGylated-peptide coating (Figure 1) that assembles through adsorptive mechanisms onto material surfaces from dilute aqueous solution to convert titanium (Ti), a lightweight and tough metal routinely used in orthopedic devices, into a fouling-resistant surface. These coatings efficiently block the adsorption of fibronectin to Ti and significantly reduce the extent of *Staphylococcus aureus* attachment and biofilm formation *in vitro*. Additionally, we investigate peptide adsorption on different materials and over a range of pH and salt concentrations to probe and elucidate the fundamental basis of the coating affinity and specificity for Ti.

## Results and Discussion

Peptide sequences with specific affinity for titanium (Ti) were identified using a combinatorial phage display technique.[21−26] Fourteen M13 phage libraries, each displaying ~$10^9$ different peptide sequences on their coat proteins, were screened for binding to Ti-6Al-4V, a Ti alloy commonly employed in orthopedic devices. Three successive screens yielded six unique peptide sequences 10−20 amino acids in length, which were synthesized with a terminal biotin group and assessed for Ti affinity using a modified ELISA. The apparent dissociation constant (or "relative $K_d$") was determined by the peptide concentration corresponding to 50% of the maximal absorbance signal and is inversely proportional to the binding affinity. This first set of peptides possessed moderate binding affinities, with $K_d$ values ranging from 0.2 to 100 $\mu$M. Peptide **1**, with a relatively weak affinity and minimal cross-reactivity with other substrate materials, was selected as a "parent" sequence from which higher affinity peptides were derived (Table 1). A series of amino acid substitutions were made to **1** and the resulting derivatives tested for binding to Ti to assess the role of specific residues in binding (Figure 2). The HKH tripeptide motif was found to significantly influence metal binding. Substitution of HKH residues with GGG resulted in a >25-fold decrease in binding strength (peptide **2** vs **1**). Based on these results, a series of synthetic peptides were designed and synthesized. Peptides **3** and **4**, containing two and three repeats of the HKH motif respectively, showed a 20- and 100-fold improvement, respectively, in binding strengths over **1**, the "parent" peptide. Peptide **4**, the strongest binding sequence, was conjugated to poly(ethylene glycol) (PEG; $M_w$ 3400). The resultant PEGylated-peptide, **5**, was subsequently characterized for its ability to coat Ti metal and confer protein and cell resistance.

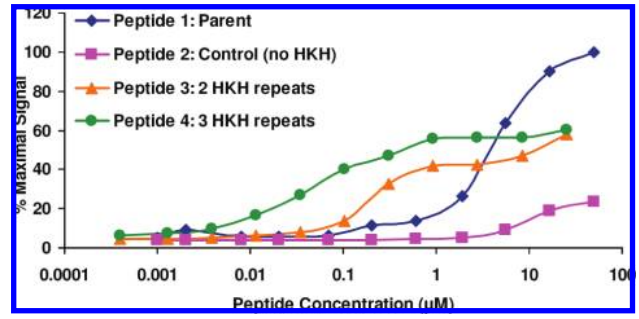


***Figure 2.*** Affinity measurements of various peptides on Ti substrates. Engineered peptides show increasing affinity with more HKH repeats. Substitution of the HKH sequence with GGG (control) results in a significant loss in affinity, demonstrating its importance for Ti binding.

***Table 1.*** Titanium-Binding Peptide (TBP) Sequences and Their Relative Ti Affinities (K* = K-Biotin)

| no. | peptide sequence | $M_w$ | Rel. $K_d$ ($\mu$M) |
|---|---|---|---|
| 1 | S**HKH**PVTPRFFVVESK* | 1895.1 | 4 |
| 2 | S**GGG**VTPRFFVVESK* | 1566.7 | >100 |
| 3 | S**HKH**GG**HKH**GSSGK* | 1440.5 | 0.2 |
| 4 | S**HKH**GG**HKH**GG**HKH**GSSGK* | 1957.1 | 0.035 |
| 5 | S**HKH**GG**HKH**GG**HKH**GSSGK-***PEG*** | 5244.1 | − |

To determine the effectiveness of surface modification, a variety of surface analytical measurements were performed on peptide-coated substrates. Coated substrates were prepared by incubating clean Ti-coated glass coverslips in 26 $\mu$M solutions of **4**, **5**, unconjugated PEG3400, or buffer alone for 2 h at RT followed by profuse washing. Static water contact angle measurements were used as a measure of surface modification. Uncoated Ti surfaces showed an angle of 7.0 ± 0.03°. Surfaces coated with **4** and **5** exhibited a significant contact angle increase to 23.7 ± 0.1° and 31.8 ± 0.3° ($p < 0.05$ and $p < 0.01$), respectively (see Supporting Information), thus confirming modification. XPS analysis of coated surfaces showed a decrease

(7) Blattler, T. M.; Pasche, S.; Textor, M.; Griesser, H. J. *Langmuir* **2006**, *22*, 5760–5769.
(8) Blummel, J.; Perschmann, N.; Aydin, D.; Drinjakovic, J.; Surrey, T.; Lopez-Garcia, M.; Kessler, H.; Spatz, J. P. *Biomaterials* **2007**, *28*, 4739–4747.
(9) Ostuni, E. O.; Chapman, R. G.; Liang, M. N.; Meluleni, G.; Pier, G.; Ingber, D. E.; Whitesides, G. M. *Langmuir* **2001**, *17*, 6336–6343.
(10) Hou, S.; Burton, E. A.; Simon, K. A.; Blodgett, D.; Luk, Y. Y.; Ren, D. *Appl. Environ. Microbiol.* **2007**, *73*, 4300–4307.
(11) Xia, N.; Hu, Y.-H.; Grainger, D. W.; Castner, D. G. *Langmuir* **2002**, *18*, 3225–3262.
(12) Kingshott, P.; Wei, J.; Bagge-Ravn, D.; Gadegaard, N.; Gram, L. *Langmuir* **2003**, *19*, 6912–6921.
(13) Scott, E. A.; Nichols, M. D.; Cordova, L. H.; George, B. J.; Jun, Y. S.; Elbert, D. L. *Biomaterials* **2008**, *29*, 4481–4493.
(14) Barber, T. A.; Gamble, L. J.; Castner, D. G.; Healy, K. E. *J. Orthop. Res.* **2006**, *24*, 1366–1376.
(15) Lopez, G. P.; Ratner, B. D.; Tidwell, C. D.; Haycox, C. L.; Rapoza, R. J.; Horbett, T. A. *J. Biomed. Mater. Res.* **1992**, *26*, 415–439.
(16) Tosatti, S.; De Paul, S. M.; Askenda, I. A.; Vande-Vondele, S.; Hubbell, J. A.; Tengvall, P.; Textor, M. *Biomaterials* **2003**, *27*, 4949–4958.
(17) VandeVondele, S.; Voros, J.; Hubbell, J. A. *Biotechnol. Bioeng.* **2003**, *82*, 784–790.
(18) Wach, J. Y.; Malisova, B.; Bonazzi, S.; Tosatti, S.; Textor, M.; Zurcher, S.; Gademann, K. *Chemistry* **2008**, *14*, 10579–10584.
(19) Dalsin, J. L.; Hu, B. H.; Lee, B. P.; Messersmith, P. B. *J. Am. Chem. Soc.* **2003**, *125*, 4253–4258.
(20) Kenan, D. J.; Walsh, E. B.; Meyers, S. R.; O'Toole, G. A.; Carruthers, E. G.; Lee, W. K.; Zauscher, S.; Prata, C. A. H.; Grinstaff, M. W. *Chem. Biol.* **2006**, *13*, 695–700.
(21) Smith, G. P. *Science* **1985**, *228*, 1315–1317.
(22) Smith, G. P.; Petrenko, V. A. *Chem. Rev.* **1997**, *97*, 391–410.
(23) Hoess, R. H. *Chem. Rev.* **2001**, *101*, 3205–3218.
(24) Dwyer, M. A.; Lu, W.; Dwyer, J. L.; Kossiakoff, A. A. *Chem. Biol.* **2000**, *7*, 263–274.
(25) Sano, K. I.; Shiba, K. *J. Am. Chem. Soc.* **2003**, *125*, 14234–14235.
(26) Sano, K.; Sasaki, H.; Shiba, K. *Langmuir* **2005**, *21*, 3090–3095.

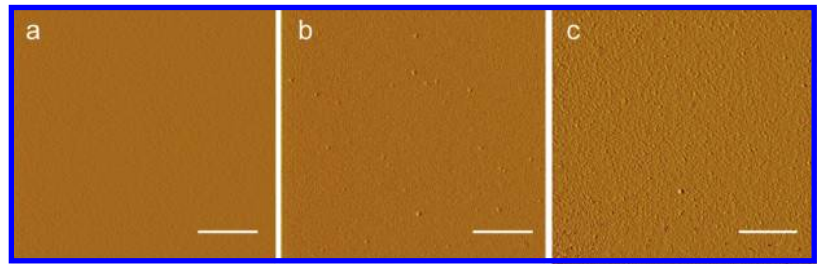


***Figure 3.*** AFM analysis of surface structures. AFM surface scans of (a) uncoated mica or mica treated with (b) 0.0026 $\mu$M or (c) 26 $\mu$M solution of **5**. The number and density of surface structures increase with concentration of the peptide solution. Scale bar = 500 nm.

in the titanium and oxygen signals and a new strong nitrogen peak at 399.9 eV, confirming the presence of an adhered peptide-based surface coating. In addition, by resolving and fitting the C1s peak, relative compositions of the different carbon bonds could be distinguished, each with a slightly different bonding energy (see Supporting Information). Three different carbon bond types, C−O, C−C, and C−H, were found for surfaces modified with **4** and **5**. As expected, **5** had a higher relative percentage of C−O bonds than **4** (38.5% vs 27.0%) due to the presence of conjugated PEG. Uncoated surfaces and surfaces coated with free PEG showed predominantly C−C/C−H bonds from surface hydrocarbons. Finally, atomic force microscopy (AFM) was used to examine surface morphology on surfaces exposed to various peptide concentrations. Freshly cleaved mica, due to its uniformity and atomic level flatness, was used in place of Ti substrates. Surfaces exposed to **5** showed highly distinct changes in surface topography dependent on peptide concentration (Figure 3). Peptide **5** adsorbed in a globular conformation to form a densely packed adlayer. Analysis of the cross-sectional profile revealed an average peptide-PEG height of 0.5 nm. Using a variety of surface characterization techniques, we have demonstrated that simple immersion of Ti substrates in a dilute aqueous peptide solution results in the rapid and spontaneous formation of a thin adherent peptide film. In all cases, surfaces incubated with free PEG alone showed little or no change in surface properties, highlighting the importance of the Ti-binding peptide domain for surface binding and functionalization.

Quartz crystal microbalance with dissipation monitoring (QCM-D) was used to investigate the real-time adsorption behavior of peptides onto Ti-coated sensors from aqueous solution. QCM-D is capable of measuring changes in adsorbed mass and viscoelastic properties of adsorbed material via differences in the frequency and decay of oscilliation, respectively.[27−29] For sufficiently rigid films, measured changes in frequency are associated with changes in adsorbed mass per area according to the Sauerbrey relation.[30,31] Exposure of Ti surfaces to **4** and **5** (26 $\mu$M in DPBS; 0.1 mg/mL) resulted in immediate binding, as evidenced by the resultant frequency ($f$) and dissipation ($D$) shifts (Figure 4, top). Adsorption occurred rapidly, reaching equilibrium in under 2 min with $\Delta f = -12.25$ Hz and $-27$ Hz for **4** and **5**, respectively. This adsorption was minimally affected by a subsequent buffer wash, indicating stable and strong binding to the Ti surfaces. The frequency shift for **5** was ~2.5 times greater than that of **4**, consistent with the fact that **5** has a molecular weight of 2.5 times that of the base peptide alone. Fitting the data to a viscoelastic Kevin−Voigt model and applying the Sauerbrey relation, we obtain a surface loading curve (Figure 4, bottom) showing equilibrium absorbed masses of 131 and 362 ng/cm$^2$ for **4** and **5**, respectively. Several studies have reported significant differences between the Sauerbrey mass and mass calculated from ellipsometry (ELM), optical waveguide lightmode spectrometry (OWLS), and surface plasmon resonance (SPR).[32−37] Unlike the optical-based techniques that

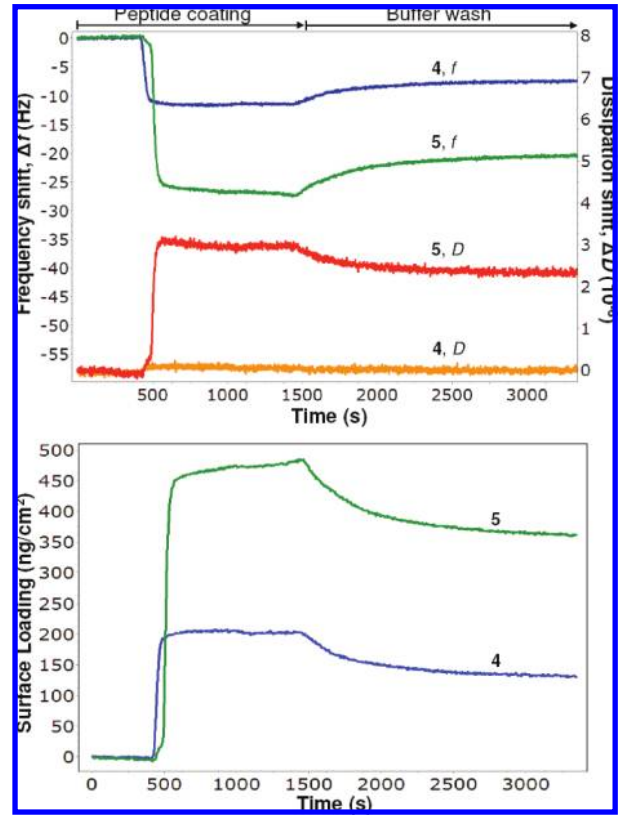


***Figure 4.*** Real-time QCM-D measurements. (Top) Observed frequency ($f$) and dissipation ($D$) shifts upon adsorption of peptides **4** and **5** on Ti crystal sensors. The additional PEG group on **5** accounts for the differences in the resultant adlayer mass and viscosity. (Bottom) Corresponding increase in adsorbed mass using the Sauerbrey relation.



(27) Rodahl, M.; Hook, F.; Fredriksson, C.; Keller, C. A.; Krozer, A.; Brzezinski, P.; Voinova, M.; Kasemo, B. *Faraday Discuss.* **1997**, 229–246.
(28) Rodahl, M.; Hook, F.; Kasemo, B. *Anal. Chem.* **1996**, *68*, 2219–2227.
(29) Rodahl, M.; Hook, F.; Krozer, A.; Brzezinski, P.; Kasemo, B. *Rev. Sci. Instrum.* **1995**, *66*, 3924–3930.
(30) Jordan, J. L.; Fernandez, E. J. *Biotechnol. Bioeng.* **2008**, *101*, 837–842.
(31) Sauerbrey, G. *Z. Phys.* **1959**, *155*, 206.
(32) Hook, F.; Voros, J.; Rodahl, M.; Kurrat, R.; Boni, P.; Ramsden, J. J.; Textor, M.; Spencer, N. D.; Tengvall, P.; Gold, J.; Kasemo, B. *Colloid Surf., B* **2002**, *24*, 155–170.
(33) Hook, F.; Kasemo, B.; Nylander, T.; Fant, C.; Sott, K.; Elwing, H. *Anal. Chem.* **2001**, *73*, 5796–5804.
(34) Halthur, T. J.; Elofsson, U. M. *Langmuir* **2004**, *20*, 1739–1745.
(35) Hemmersam, A. G.; Foss, M.; Chevallier, J.; Besenbacher, F. *Colloid Surf., B* **2005**, *43*, 208–215.

measure the "dry" adsorbed mass, QCM-D measures the change in total coupled mass, including water associated with the film hydration layer and/or water trapped in cavities in the film.[34,38] The observed mass difference between QCM-D and the optical techniques has been found to vary widely depending on the type of protein and the structure of the protein layer formed at the sensor/liquid interface.[32] However, because of the small size of **4**, we can assume minimal contribution by water associated with the adlayer. Assuming that **4** is spherical with a molecular weight of 1957 Da and diameter of 0.5 nm (as determined from AFM), we are able to estimate an ideal close packed amount of peptide to be 152 ng/cm$^2$, within 16% of the experimental value, suggesting that we have a close-to-monolayer coating. It is possible that each peptide molecule undergoes some conformation change (e.g., spreading) upon adsorption and hence may occupy a larger area than theoretically indicated. In addition, using the surface loading measurements, we can estimate a surface coverage of $\sim 4.03 \times 10^{16}$ molecules/cm$^2$, assuming the formation of a complete monolayer. Since the peptide and PEGylated-peptide show similar adsorption behaviors and surface coverages based on AFM and QCM-D data, we can estimate similar PEGylated peptide coverages. A previous study using a physisorbed PLL(20)-g[3.5]-PEG(2 KDa)/PEG(3.4 KDa)-Biotin system reports a similar maximal surface coverage of $\sim 2.4 \times 10^{16}$ molecules/cm$^2$.[39]

It is a well-known fact that protein adsorption depends strongly on the type of proteins in the mixture, the "Vroman effect", temperature, ionic strength, and pH.[40−42] To elucidate the mechanism by which the peptide coating interacts with Ti surfaces, QCM-D adsorption studies were repeated in aqueous buffer solutions of various pH and ionic strengths. The resultant frequency changes upon exposure of Ti substrates to **4** at three pH values (3, 7.4, and 11) and three NaCl concentrations (50, 100, and 400 mM) are presented in Figure 5. Peptide adsorption behavior varied significantly with pH, and maximal adsorption was observed in a pH 7.4 buffer. At pH 3, when the negative surface charge of Ti (IEP $\sim$4.7−6.2) is decreased, adsorption is reduced by over 50%.[43] At this low pH, since the Ti surface is less negative and the two basic residues histidine (IEP $\sim$6.0) and lysine (IEP $\sim$10.5) are largely protonated, electrostatic interactions are considerably reduced. At pH 11, where H (IEP $\sim$6.0) and K (IEP $\sim$10.5) are largely deprotonated, adsorption of **4** on Ti is almost negligible. The Ti-binding peptide bears little positive charge, and thus minimal electrostatic interaction with the surface is expected. Similarly, high ionic strength conditions where electrostatic double layer interactions are reduced should result in compromised peptide adhesion and monolayer stability. Figure 5 shows this inverse relationship between peptide binding and buffer NaCl concentration. Exposure to a 400 mM high salt buffer resulted in a >65% reduction in the frequency signal as compared to a low salt buffer. These results suggest that the mechanism for assembly of **4** onto Ti is most likely electrostatic adsorption. However, because adsorption is not completely eliminated despite ionic strength changes, hydrogen bonding and perhaps even surface topology may also play a part in influencing peptide binding on Ti.

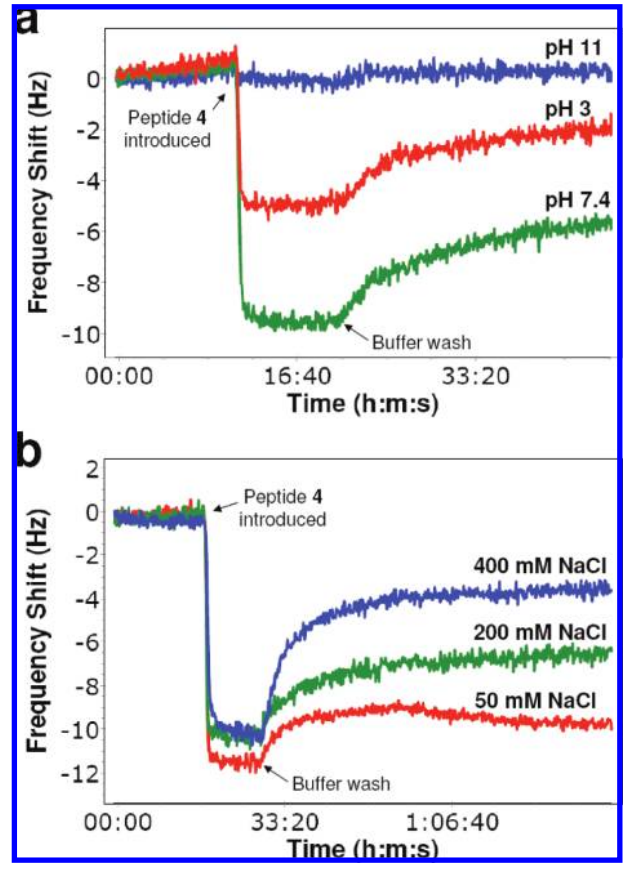


***Figure 5.*** QCM-D measurements of peptide binding at various (a) pH values and (b) buffer ionic strengths. Extreme pH values and high salt concentrations resulted in reduced binding of peptide **4** onto Ti, which suggests that electrostatic adsorption is largely responsible for coating assembly.

The binding specificity of the peptide coating was determined by monitoring the adsorption of **4** on QCM-D sensors coated with various materials: polystyrene (PS), gold (Au), silicon dioxide ($SiO_2$), stainless steel (SS), and Ti. Exposure of surfaces to peptides results in immediate adsorption in all cases, as evidenced by a rapid decrease in the frequency signals (Figure 6). Upon washing with buffer, the frequency signal gradually recovers over time, indicating desorption or washing off of weakly bound peptide. In the case of PS and Au surfaces, the frequency eventually returns to baseline, indicating almost complete loss of peptide. On Ti, however, the signal reaches stable equilibrium, corresponding to a finite amount of bound peptide remaining on the surface. Peptide adsorption is also observed on SS and $SiO_2$ surfaces, albeit to a lesser extent than on Ti, as evidenced by smaller equilibrium frequency shifts. ELISAs on beads of different materials (oxinium, SS, PS, and Ti) reveal similar selectivities (see Supporting Information). Peptide **4** shows cross-reactivity with some non-titanium substrates, namely metals with a naturally occurring surface oxide layer, and negligible adsorption on others, such as Au and PS. This selective binding of **4** suggests that the peptide recognizes a common structure shared by Ti, SS, and $SiO_2$, since these metals are oxidized under ambient conditions. However, electrostatic interactions are not sufficient to explain the preferred binding of **4** to Ti over the other metals since the

(36) Keller, C. A.; Glasmastar, K.; Zhdanov, V. P.; Kasemo, B. *Phys. Rev. Lett.* **2000**, *84*, 5443–5446.
(37) Larsson, C.; Rodahl, M.; Hook, F. *Anal. Chem.* **2003**, *75*, 5080–5087.
(38) Caruso, F.; Furlong, D. N.; Kingshott, P. *J. Colloid Interface Sci.* **1997**, *186*, 129–140.
(39) Schoch, R. B.; Cheow, L. F.; Han, J. *Nano Lett.* **2007**, *7*, 3895–3900.
(40) Vroman, L. *Nature* **1962**, *196*, 476–477.
(41) Lee, S.; Spencer, N. D. *Langmuir* **2008**, *24*, 9479–9488.
(42) Tsapikouni, T. S.; Missirlis, Y. F. *Colloids Surf., B* **2007**, *57*, 89–96.
(43) Parks, G. A. *Chem. Rev.* **1965**, *65*, 177–198.

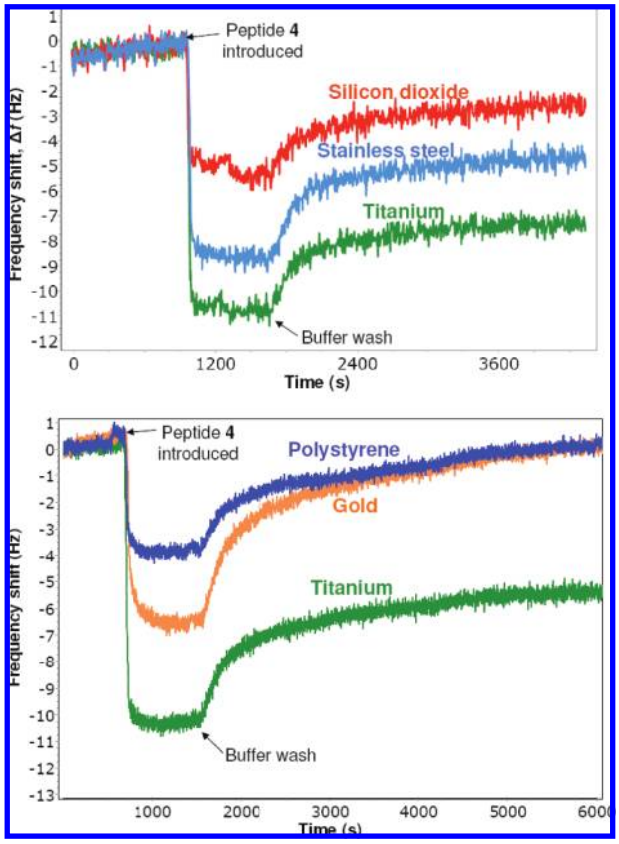


***Figure 6.*** Determination of peptide specificity using QCM-D. **4** shows preferred binding to Ti, with some cross-reactivity with SS and $SiO_2$, and very weak binding to PS and Au.

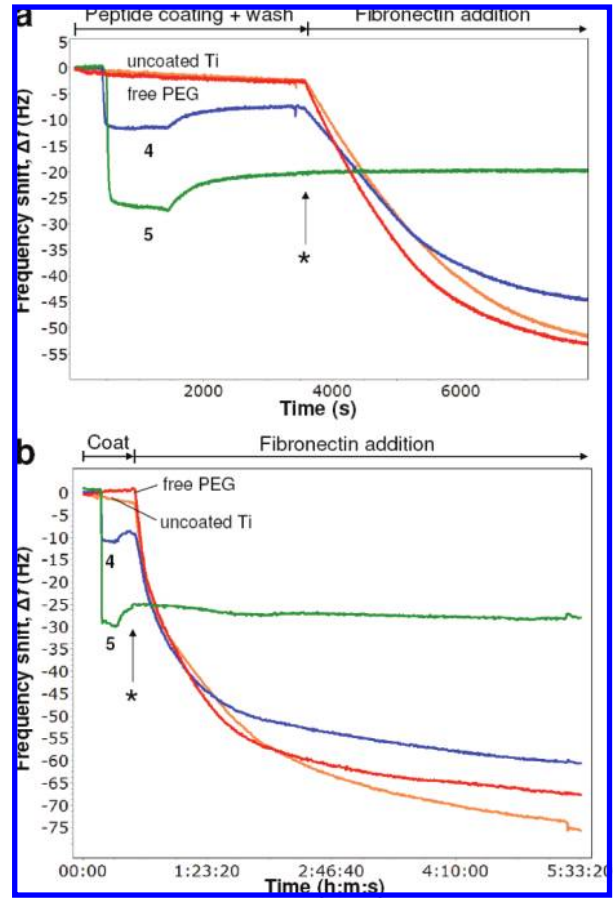


***Figure 7.*** QCM-D frequency shifts with (a) short-term (1.5 h) and (b) long-term (5 h) surface exposure to a 4 $\mu$g/mL fibronectin solution. Only surfaces coated with the PEGylated-peptide, **5**, show strong resistance to Fn adsorption. Fn resistance, even at long exposure times, demonstrate the robustness of the coating against displacement by serum protein. Fn addition is marked (*).

surface charges of Ti, SS (IEP ~4.3), and $SiO_2$ (IEP ~2.2) would suggest that **4** will adhere better on SS and $SiO_2$.[43,44] It is likely that other factors, such as material-specific crystal structure or localized surface charges, also contribute to the binding selectivity of the peptide coating.

Prevention of implant-associated infections is contingent upon the inhibition of both protein and bacterial adherence onto implant surfaces.[45−47] Consequently, QCM-D was used to measure fibronectin binding on coated and uncoated Ti to assess the capability of the peptide coatings to resist protein adsorption. **4**, **5**, or PEG alone were introduced over Ti-coated sensors and allowed to interact with surfaces. The resulting frequency shifts (Figure 7a) indicate the adsorption of **4** and **5** but not PEG onto substrates. Fibronectin (Fn; 4 $\mu$g/mL) was subsequently introduced over the "precoated" Ti surfaces, and the extent of Fn binding was assessed over 1.5 h. As expected, only the surface initially exposed to **5** shows inhibition of Fn adsorption, as seen from a lack of change in the frequency signal. The uncoated, **4**-coated, and PEG-coated surfaces show large frequency shifts corresponding to ~0.61−0.87 $\mu$g/cm$^2$ of adsorbed Fn. Next, to determine the robustness of the coating and its ability to resist displacement by serum proteins over longer periods, coated surfaces were challenged with Fn over a period of 5 h. Again, only the Ti surface initially coated with **5** shows inhibition of Fn adsorption (Figure 7b). Over 5 h, only a slight displacement of **5** by Fn is observed, as indicated by a small frequency shift of $\Delta f = -3.38$ Hz. This corresponds to a final adsorbed Fn mass of 55 ng/cm$^2$. Uncoated and control surfaces show significant Fn adsorption ranging from 0.87 to 1.24 $\mu$g/cm$^2$, more than 150-fold the amount adsorbed on **5**-coated surfaces. These results confirm the nonfouling nature of **5** and demonstrate its ability to confer protein resistance on Ti surfaces, even when presented with a protein challenge over a period of several hours.

Finally, to determine the effectiveness of the functionalized peptides as a bacteriophobic implant coating, we investigated the ability of **5** to inhibit *Staphylococcus aureus* colonization on Ti surfaces. This pathogen is responsible for a significant proportion of infections associated with medical devices and is often transferred to the implant during handling.[45,48,49] *S. aureus* strain MZ100 was added to coated Ti substrates at a concentration of ~5 × 10$^7$ CFUs/well, ~10 000 times typical counts on human skin. By 4 h, a thick layer of adhered cells was observed on uncoated Ti and surfaces treated with PEG or **4** (Figure 8a−d). The surface treated with **5**, however, had very few adhered bacteria, with most present as individual cells. Surfaces

(44) Fukuzaki, S.; Urano, H.; Nagata, K. *J. Ferment. Bioeng.* **1995**, *80*, 6–11.
(45) Gristina, A. G. *Science* **1987**, *237*, 1588–1595.
(46) Arciola, C. R.; Bustanji, Y.; Conti, M.; Campoccia, D.; Baldassarri, L.; Samori, B.; Montanaro, L. *Biomaterials* **2003**, *24*, 3013–3019.
(47) Maddikeri, R. R.; Tosatti, S.; Schuler, M.; Chessari, S.; Textor, M.; Richards, R. G.; Harris, L. G. *J. Biomed. Mater. Res A* **2008**, *84*, 425–435.
(48) Arciola, C. R.; Campoccia, D.; Montanaro, L. *Expert Rev. Mol. Diagn.* **2002**, *2*, 478–484.
(49) Harris, L. G.; Richards, R. G. *Injury* **2006**, *37* (2), S3–14.

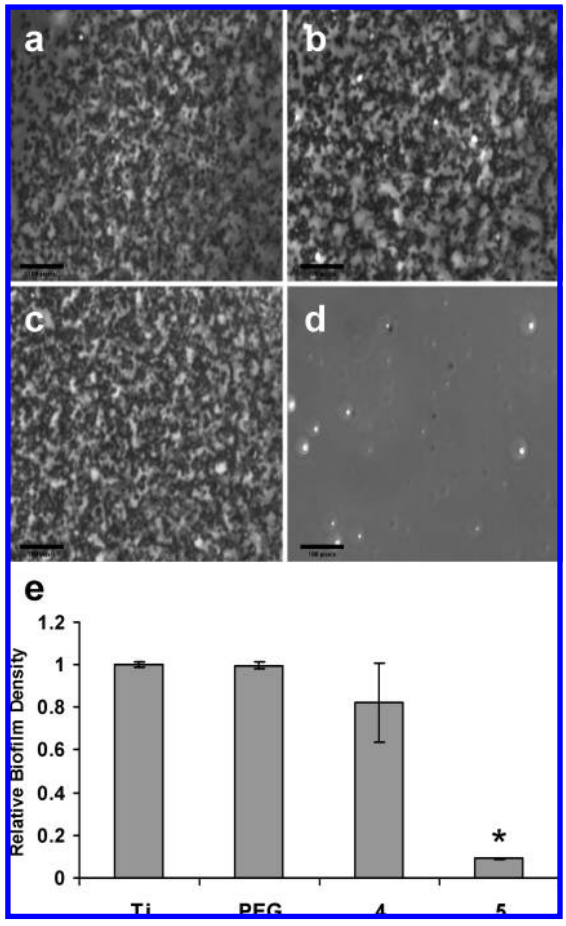


***Figure 8.*** Assessment of bacteria inhibition. Phase-contrast images showing *S. aureus* adhesion following a 4 h incubation on (a) uncoated Ti, (b) PEG3400-coated Ti, (c) **4**-coated Ti, and (d) **5**-coated Ti. Scale bar = 35 $\mu$m. (e) Biofilm formation in response to various surface coatings quantified using a crystal violet assay. Surfaces treated with **5** show significantly reduced biofilm density over the other three surfaces ($n = 3$; $^*P < 0.01$).

were also assayed for biofilm formation using a modified version of the standard microtiter plate assay.[50] Surfaces pretreated with the bacteriophobic coating, **5**, showed a 10-fold decrease in biofilm density over all other surfaces, as determined by the optical density measured at 550 nm (Figure 8e). It has been previously shown that only beyond a critical inoculum of $10^5$ organisms per gram of tissue is the host immune defense threatened with a high risk of infection.[51] Thus, the few bacterial cells that remain adhered on the PEGylated-peptide surface may be eradicated by the host immune system and not develop into an infection. This will need to be tested *in vivo* in a future experiment. These results demonstrated the ability of **5** to resist adhesion of bacteria and subsequent biofilm formation, even when challenged with a high inoculum concentration.

## Conclusion

In summary, we have developed and evaluated a nonfouling PEGylated-peptide coating for the prevention of nonspecific interactions on titanium metal surfaces. A high affinity Ti-binding peptide was identified via combinatorial phage display and amino acid substitution techniques. The candidate peptide sequence, **4**, was enriched with HKH residues and showed cross-reactivity with other metal oxides. QCM-D analysis of the binding behavior at various pH and ionic strengths revealed that electrostatic interactions play a major role in the assembly of the peptide coating. The PEGylated-peptide coating was then characterized and shown to confer resistance to protein and bacterial adherence on Ti. Treatment with **5** significantly decreased the amount of adherent *S. aureus* in comparison to bare Ti or Ti treated with unconjugated PEG. The development of surface coatings that control specific biological interactions on Ti is likely to significantly improve the long-term efficacy and performance of Ti orthopedic devices. This approach offers several advantages for use in the clinic, including the capacity to apply coatings to materials of complex shapes and sizes by simple immersion under mild, aqueous conditions at the point of care. Furthermore, as we have previously shown, the modular nature of this platform presents a general approach for the directed assembly and organization of other biological and chemical mediators on a variety of target materials ranging from metal to plastic to ceramic.[52−54]

**Acknowledgment.** We thank E. Shaw at the MIT CMSE for her assistance with XPS. The authors also thank Drs. Robin Hyde-DeRuyscher and Wayne Beyer (Affinergy) for their contributions to the isolation and design of the Ti binding peptides. This work was financially supported by the National Institutes of Health (Grant No. AR054872-01). M.W.G. and D.J.K. are cofounders of Affinergy.

**Supporting Information Available:** Experimental methods, surface analytical data (XPS, contact angle), and ELISA peptide specificity measurements (PDF). This material is available free of charge via the Internet at http://pubs.acs.org.

JA9020827

(50) Shanks, R. M. Q.; Donegan, N. P.; Graber, M. L.; Buckingham, S. E.; Zegans, M. E.; Cheung, A. L.; O'Toole, G. A. *Infect. Immun.* **2005**, *73*, 4596–4606.
(51) Clifford, R. P. In *AO Principles of Fracture Management*; Rüedi, T. P., Murphy, W. M., Eds.; AO Publishing: Stuttgart, 2000; pp 617−638.
(52) Meyers, S. R.; Hamilton, P. T.; Walsh, E. B.; Kenan, D. J.; Grinstaff, M. W. *Adv. Mater.* **2007**, *19*, 2492–2498.
(53) Meyers, S. R.; Kenan, D. J.; Grinstaff, M. W. *ChemMedChem* **2008**, 1645–1648.
(54) Meyers, S. R.; Khoo, X.; Huang, X.; Walsh, E. B.; Grinstaff, M. W.; Kenan, D. J. *Biomaterials* **2009**, *30*, 277–286.